Kristensen, T., Wetsel, R. A., & Tack, B. F. (1986) *J. Immunol. 136*, 3407-3411.
Kristensen, T., D'Eustachio, P., Ogata, R. T., Chung, L. P., Reid, K. B. M., & Tack, B. F. (1987) *Fed. Proc., Fed. Am. Soc. Exp. Biol. 46*, 2463-2469.
Leonard, W. J., Depper, F. M., Kanehisa, M., Kronke, M., Peffer, N. J., Svetlik, P. B., Sullivan, M., & Greene, W. C. (1985) *Science (Washington, D.C.) 230*, 633-639.
Leytus, S. P., Kurachi, K., Sakariassen, K. S., & Davie, E. W. (1986) *Biochemistry 25*, 4855-4863.
Lozier, J., Takahashi, N., & Putnam, F. W. (1984) *Proc. Natl. Acad. Sci. U.S.A. 81*, 3640-3644.
Maeda, N. (1985) *J. Biol. Chem. 260*, 6698-6709.
Maniatis, T., Fritsch, E. F., & Sambrook, J. (1982) *Molecular Cloning: A Laboratory Manual*, Cold Spring Harbor Laboratory, Cold Spring Harbor, NY.
Maxam, A. M., & Gilbert, W. (1980) *Methods Enzymol. 65*, 499-560.
Mole, J. E., Anderson, J. K., Davison, E. A., & Woods, D. E. (1984) *J. Biol. Chem. 269*, 3407-3412.
Morley, B. J., & Campbell, R. D. (1984) *EMBO J. 3*, 153-157.
Nagasawa, S., & Stroud, R. M. (1980) *Mol. Immunol. 17*, 1365-1372.
Nagasawa, S., Mizuguchi, K., Ichihara, C., & Koyama, J. (1982) *J. Biochem. (Tokyo) 92*, 1329-1332.
Okayama, H., & Berg, P. (1982) *Mol. Cell. Biol. 2*, 161-170.
Okayama, H., & Berg, P. (1983) *Mol. Cell. Biol. 3*, 280-289.
Padgett, R. A., Gravowksi, P. J., Konarska, M. M., & Sharp, P. A. (1985) *Trends Biochem. Sci. (Pers. Ed.) 10*, 154-157.
Perkins, S. J., Chung, L. P., & Reid, K. B. M. (1986) *Biochem. J. 233*, 799-807.
Reid, K. B. M., & Gagnon, J. (1982) *FEBS Lett. 137*, 75-79.
Reid, K. B. M., Bentley, D. R., Campbell, R. D., Chung, L. P., Sim, R. B., Kristensen, T., & Tack, B. F. (1986) *Immunol. Today 7*, 230-234.
Rigby, P. W. J., Dieckmann, M., Rhodes, C., & Berg, P. (1977) *J. Mol. Biol. 113*, 237-251.
Sanger, F., Nicklen, S., & Coulson, A. R. (1977) *Proc. Natl. Acad. Sci. U.S.A. 74*, 5463-5467.
Scharfstein, J., Ferreira, A., Gigli, I., & Nussenzweig, V. (1978) *J. Exp. Med. 148*, 207-222.
Shimuzu, A., Kondo, S., Takeda, S., Yodai, J., Ishida, N., Sabe, H., Osawa, H., Diamantstein, T., Nikaido, T., & Honjo, T. (1985) *Nucleic Acids Res. 13*, 1505-1516.
Spycher, S. E., Nick, H., & Rickli, E. E. (1986) *Eur. J. Biochem. 156*, 49-57.
Staden, R. (1980) *Nucleic Acids Res. 8*, 3673-3694.
Staden, R. (1982a) *Nucleic Acids Res. 10*, 4731-4751.
Staden, R. (1982b) *Nucleic Acids Res. 10*, 2951-2961.
Takahashi, S., Takahashi, M., Kaidoh, T., Natsuume-Sakai, S., & Takahashi, T. (1984) *J. Immunol. 132*, 6-8.
Tosi, M., Colomb, M., & Meo, T. (1986) 6th International Congress of Immunology, Toronto, Canada, Abstr. 2.54.7, p 198.
Watson, M. E. E. (1984) *Nucleic Acids Res. 12*, 5145-5164.

Molecular Mechanics and Dynamics Calculations on $(dA)_{10}\cdot(dT)_{10}$ Incorporating Distance Constraints Derived from NMR Relaxation Measurements†

Ronald W. Behling,‡,§ Shashidhar N. Rao,‖ Peter Kollman,‖ and David R. Kearns*,‡
Department of Chemistry, University of California at San Diego, La Jolla, California 92093, and Department of Pharmaceutical Chemistry, School of Pharmacy, University of California, San Francisco, California 94143
Received November 24, 1986; Revised Manuscript Received March 9, 1987

ABSTRACT: Structural constraints derived from proton NMR relaxation measurements on poly(dA)·poly(dT) in the form of interproton separations and orientation have been combined with molecular mechanics and annealed molecular dynamics calculations to derive a model for the solution-state structure of this molecule. Three different possible starting configurations, including the standard A and B forms of Arnott and Hukins [Arnott, S., & Hukins, D. W. L. (1972) *Biochem. Biophys. Res. Commun. 47*, 1506-1509] and the heteronomous (H) structure [Arnott, S., Chandrasekaran, R., Hall, I. H., & Puigjaner, L. C. (1983) *Nucleic Acids Res. 11*, 4141-4155], were examined. Both the B- and H-DNA structures converged to the same B-like structure (approximately C2′-endo conformation on both the A and T sugars, glycosidic bond torsional angle of 63-73°) with the same energies and average helical parameters that gave good fits of the NMR relaxation rates. This model also accounts for the experimental observation [Behling, R. W., & Kearns, D. R. (1986) *Biochemistry 25*, 3335-3346] that the AH2 proton interacts more strongly with the H1′ sugar proton on the T strand than on the A strand. Although the helix repeat angle (39°) is larger than that for standard B-DNA (36°), this does not result in a significantly smaller minor groove, as monitored by the interstrand P-P separation. Calculations starting with the A-DNA structure lead to a very high energy structure that gave a poorer fit of the NMR data.

Poly(dA)·poly(dT) is a particularly interesting simple sequence DNA because $A_n\cdot T_n$ stretches occur commonly in natural DNA and they appear to have unusual properties (Trifonov & Sussman, 1980). A·T-rich DNAs are known to have low melting points (Sober & Harte, 1970), but stretches of $(dA)_n\cdot(dT)_n$ are remarkably resistant to DNase I and DNase II (Drew & Travers, 1984, 1985). It has been suggested (Drew & Travers, 1984) that this resistance to nuclease digestion is because the minor groove in poly(dA)·poly(dT) is

† This work was supported by the National Science Foundation (Grant PCM 83-03374 to D.R.K.).
‡ University of California at San Diego.
§ Present address: AT&T Bell Laboratories, Murray Hill, NJ 07974.
‖ University of California, San Francisco.

0006-2960/87/0426-4674$01.50/0

especially narrow, which correlates with the substantially lower average base pair per helical turn in poly(dA)·poly(dT) compared to most DNAs (Klug et al., 1980; Pack & Wang, 1981). A_n·T_n stretches appear to be the loci of bending in trypanosome kinetoplast DNA (Marini et al., 1982; Wu & Crothers, 1984). The behavior of poly(dA)·poly(dT) is also unusual and different from the sequence isomer poly(dA-dT) and other DNAs with respect to thermodynamics and kinetics of drug binding (Wilson et al., 1985). To account for their observations, Wilson et al. (1985) suggest that water molecules tightly bound to the minor groove might be responsible for the unusual behavior of poly(dA)·poly(dT). This receives some support from the observation (Dickerson et al., 1982; Kopka et al., 1983) that in DNA crystals the water in the minor groove is more structured around A·T than G·C base pairs. If Wilson's suggestion is true, then hydration differences might also have a pronounced affect on the interaction of $(dA)_n\cdot(dT)_n$ sequences with proteins (including nucleases). The possibility that the unusual solution-state physical and biochemical properties of poly(dA)·poly(dT) might instead be due to an unusual conformation is suggested by the work of Arnott et al. (1983). On the basis of their analysis of the fiber X-ray diffraction studies, they propose that poly(dA)·poly(dT) can adopt a heteronomous structure (H-DNA) where all nucleotides in the A strand adopt a C3′-endo conformation, whereas in the thymine strands they remain C2′-endo (Arnott et al., 1983). Rao and Kollman (1985) suggest, in contrast, that any sugar repuckering of poly(dA)·poly(dT) corresponds to a substantial population of dT(C3′-endo)·dA(C2′-endo) rather than the dT(C2′-endo)·dA(C3′-endo) conformation of Arnott et al. (1983). That conformations with significant C3′-endo population might persist in solution is suggested by Raman measurements that have been interpreted to indicate that at low temperatures poly(dA)·poly(dT) contains a substantial C3′-endo sugar conformation in contrast with B-form DNA, where the sugar conformation is pure C2′-endo (Thomas & Peticolas, 1983). Room temperature Raman measurements indicate a C2′-endo/C3′-endo ratio of ~80/20 (Wartell & Harrell, 1986), and resonance Raman measurements suggest that the stacking of the bases in the adenine strand is more "RNA-like" (Jolles et al., 1985). It has recently been suggested (Pattabiraman, 1986) that poly(dA)·poly(dT) might adopt a parallel right-handed double-helical structure with reverse Watson–Crick pairing, but this possibility has been eliminated by our two-dimensional nuclear Overhauser effect (2D NOE) studies (Behling & Kearns, 1986). X-ray diffraction studies indicate that poly(dA)·poly(dT) is also unusual in that it cannot be converted to an A form in the fibers under conditions where many other DNA polymers do (Leslie et al., 1980).

We recently performed one- and two-dimensional (1D and 2D) NMR relaxation measurements on 60 base pair (bp) fragments of poly(dA)·poly(dT) (Behling & Kearns, 1985a,b, 1986) to establish some of the qualitative structural features and to provide a set of NMR relaxation rates that could be used to quantitatively evaluate the structure of this molecule. In that study we established that the poly(dA)·poly(dT) strands are structurally equivalent, or nearly so, and that the average conformations of the sugar groups in both strands were close to C2′-endo. From these studies we generated a set of constraints on various interproton distances that might be used in a structure search. Sarma et al. (1985a,b) independently arrived at similar conclusions on the basis of 1D NOE studies on 200 ± 50 bp DNA samples, and they too convincingly demonstrated that the sugar groups were not C3′-endo.

In this study, we develop a model for the poly(dA)·poly(dT) structure by combining the structural constraints derived from our NMR measurements with molecular mechanics and annealed molecular dynamics based on the AMBER program. Three different starting structures were used in the calculations: the B form and A form derived from X-ray diffraction measurements on DNA fibers (Arnott & Hukins, 1972) and the heteronomous structure proposed by Arnott et al. (1983). The latter structure was included because it gave the best account of the X-ray fiber diffraction data of the poly(dA)·poly(dT) fibers. The B-DNA structure was examined because we found that it gave a good account of the qualitative aspects of the NMR relaxation data (Behling & Kearns, 1985a, 1986), and the A-form structure was included to see how the incorporation of the NMR-derived structural constraints would be accommodated with a starting structure that gave a poor fit of the NMR data. We find that starting with either the heteronomous model (Arnott et al., 1983) or the standard B-type helix (Arnott & Hukins, 1972), energy minimization with annealed molecular dynamics (both including NMR constraints), leads to the same B-type structure. Analogous calculations starting with the A-form DNA resulted in a highly perturbed A-like structure (both A and T sugars in approximately C2′-endo conformation), with an unacceptably high energy.

Materials and Methods

Proton relaxation measurements reported previously (Behling & Kearns, 1985a,b, 1986) provide information about *both* interproton distances *and* orientation of the interproton vectors relative to the DNA helix axis in ~60 base pair (bp) fragments of poly(dA)·poly(dT). This arises from the fact that when a molecule, such as 60-bp DNA, undergoes anisotropic rotational diffusion, the cross-relaxation rates depend both on the interproton separation and on the orientation of the interproton vector relative to the axis (Woessner, 1962; Woessner et al., 1969; Mirau et al., 1985; Behling & Kearns, 1986). For a given relaxation rate, there are many possible combinations of internuclear separation and orientation that would be acceptable, and therefore from our NMR measurements, we constructed contour maps of allowed combinations of distance and orentation (Behling & Kearns, 1986), and two examples are shown in Figure 1. In this study, these constraints on the interproton geometries have been included in molecular mechanics and annealed molecular dynamics calculations to generate structures that are compatable with NMR data and at the same time satisfy energetic constraints introduced by the molecular mechanics calculations.

Since it was impractical to do calculations on a 60 base pair fragment of DNA, the calculations were carried out on the decamer $(dA)_{10}\cdot(dT)_{10}$ with the molecular mechanics program AMBER,[1] Version 3.0. All energy minimization and dynamics calculations were done on the CRAY X-MP/48 computer at the UCSD Supercomputer Center.

The calculations started with coordinates for A-, B-, or H-(heteronomous) DNA derived from the X-ray diffraction studies of Arnott et al. (1972, 1983). Protons were added to the X-ray structures by using standard bond lengths and angles. The force-field parameters used in the calculations were those reported previously (Weiner et al., 1986), and *all* DNA

[1] AMBER 2.0 and 3.0 UCSF has been largely developed by U. C. Singh, with contributions by Scott Weiner, Jim Caldwell, D. Case, and G. Seibel.

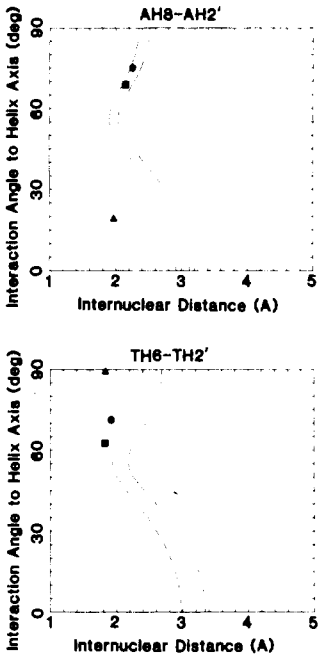

FIGURE 1: Contour plots showing the allowed combinations of internuclear distances and angles to the helix for the AH8–AH2′ and the TH6–TH2′ interactions in poly(dA)·poly(dT). The allowed geometries, those which fall between the two contour lines on the plot, fit the cross-relaxation rate σ between the two interacting protons.

protons were explicitly included in the calculations. The energy function is given by (Weiner et al., 1984)

$$E_{\text{TOTAL}} = \sum_{\text{bonds}} K_r(r - r_{\text{eq}})^2 + \sum_{\text{angles}} K_\theta(\theta - \theta_{\text{eq}})^2 + \sum_{\text{dihedrals}} \frac{V_n}{2}[1 + \cos(n\theta - \gamma)] + \sum_{i<j}\left(\frac{A_{ij}}{R_{ij}^{12}} - \frac{B_{ij}}{R_{ij}^{6}} + \frac{q_i q_i}{\epsilon R_{ij}}\right) + \sum_{\text{H-bonds}}\left(\frac{C_{ij}}{R_{ij}^{12}} - \frac{D_{ij}}{R_{ij}^{10}}\right) \quad (1)$$

The dielectric constant (ϵ) was set equal to R_{ij}, the interatomic distance (Weiner et al., 1984). The hydrogen bonds in the Watson–Crick base pairs were given a 10–12 hydrogen bond potential with a well depth of 0.5 kcal/mol. No counterions or solvent water molecules were included in the calculations, and all atoms were included in nonbonded interactions (i.e., no nonbonded cutoff). The net charge per base, −1, is distributed over the phosphate group and the sugar residues. The structures were energy-minimized with steepest-descent and conjugate gradient algorithms in Cartesian coordinate space until the rms energy gradient was less than 0.09 kcal mol^{-1} Å^{-1} (Weiner & Kollman, 1981; Kollman et al., 1982; Weiner et al., 1984).

The calculations proceeded by first energy minimizing the starting X-ray structures to obtain minimized structures based on the all-atom potentials. These structures provided starting structures for the next energy minimization calculations in which the distance constraints determined from the NMR measurements on poly(dA)·poly(dT) were incorporated. The distance constraints were included as harmonic potentials with target equilibrium distances, r_{eq}, chosen to fit the NMR data, and the constrained distances were treated as pseudobonds in the potential energy function (eq 1). The force constant for this harmonic potential was chosen to be 25 kcal/mol. While this is small compared to the ~300 kcal/mol force constant for a C–C bond, it was found adequate to ensure that the resulting structures were consistent with the NMR measurements. Nine proton–proton interactions per base pair obtained from NMR measurements on poly(dA)·poly(dT) were included as constrained distances in the energy minimizations (Behling & Kearns, 1986). These are the AH2–AH2, AH8–AH1′, AH8–AH2′, AH8–AH2″, TH6–TH1′, TH6–TH2′, TH6–TH2″, AH1′–AH2″, and TH1′–TH2″ interactions.

Because of the anisotropic rotational diffusion of 60-bp DNA, the cross-relaxation rate calculated for a given proton–proton dipolar interaction depends on *both* the interproton distance *and* the orientation of the interproton vector with respect to the helix axis (Woessner et al., 1969; Behling & Kearns, 1985a, 1986), and therefore, it is necessary to continually readjust the target equilibrium distance, r_{eq}, for each pair of interacting protons (interproton constraint) as the orientation of the interproton vector relative to the helix axis changed during the refinement process (see Figure 1). The AMBER program was accordingly modified to adjust the target equilibrium interproton distance according to the angle of the interproton vector with respect to the helix axis. After each cycle of the energy minimization procedure, the helix axis was determined, and the orientation of the interproton vector relative to the helix axis was calculated. The target equilibrium distance, r_{eq}, was then redetermined from the calculated dependence of the relaxation rate on orientation (Woessner, 1962; Woessner et al., 1969; Behling & Kearns, 1986). The minimization then proceeded with the new r_{eq} values. In some instances, the value of r_{eq} changed by as much as 0.5 Å as the orientation of the interproton vector relative to the helix axis changed during the energy minimization. However, in most cases, the change in the target r_{eq} values was 0.2–0.3 Å. Because the A or T residues on each strand in poly(dA)·poly(dT) are all equivalent, there is some ambiguity in the calculation as to the target intermolecular separation that should be used. For example, the observed AH8–AH1′ interaction could be due to an *intra-* or *inter*nucleotide interaction. When such ambiguities arose, we assumed that the observed relaxation rate is due to only one of the two possible interactions and choose that one to be the one with the shorter interproton separation in the starting structure (e.g., in B-DNA the AH8–AH1′ *inter*nucleotide separation is shorter than the *intra*nucleotide separation). At the end of the calculation the initial assumption could be checked to confirm that it was still valid.

After a structure was energy minimized with the NMR distance constraints in place, the distance constraints were removed, and the structure was reminimized. This "relaxed" structure could then be compared with the structure obtained from the unconstrained energy minimization of the starting X-ray structure and the structure obtained with NMR constraints.

The nine energy-minimized structures generated above also provided the starting coordinates for annealed molecular dynamics calculations (McCammon et al., 1977). In these calculations the molecule is heated and allowed to equilibrate at some higher temperature and then slowly cooled to avoid trapping in some local minimums. In our calculations, the energy-minimized structures were heated to 100 K and held at this temperature for 0.5 ps. The temperature was then lowered from 100 to 5 K over a time period of 5 ps. Following the annealing, the resulting structure was again energy minimized to confirm that it was the lowest energy structure possible in this potential well. As expected, the minimization took only a few steps because the structures were already close to their minimum energies at the end of the cooling step.

Table I: Comparison of Total Energies of Structures Obtained by Carrying Out Molecular Mechanics and Annealed Molecular Mechanics Calculations on A-DNA (Arnott & Hukins, 1972), B-DNA (Arnott & Hukins, 1972), and H-DNA (Arnott et al., 1983) Models for $(dA)_{10}\cdot(dT)_{10}$

	structure[a]								
	B_{NC}	B_{NMR}	B_{RE}	A_{NC}	A_{NMR}	A_{RE}	H_{NC}	H_{NMR}	H_{RE}
energy (kcal/mol) after molecular mechanics	−575	−527 (−489)[b]	−575	−561	−338 (−322)[b]	−571	−557	−530 (−506)[b]	−573
energy of structure after annealed molecular dynamics	−578	−544 (−534)[b]	−576	−567	−448 (−429)[b]	−574	−561	−546 (−537)[b]	−577

[a] For a discussion of the various structures, see text. [b] The values in parentheses are the energies of structures including the potentials added to introduce the NMR constraints.

Table II: Analysis of B-Form Structures for $(dA)_{10}\cdot(dT)_{10}$ Obtained by Combined Molecular Mechanics and Annealed Molecular Dynamics Calculations

structure/parameter	starting X-ray (B_{XRAY})	minimized, no constraints ($B_{NC/a}$)	minimized, 25-kcal constraints ($B_{NMR/a}$)	relaxed from 25-kcal constraints ($B_{RE/a}$)
energy (kcal/mol)		−578	−544 (−534)[a]	−576
rms structure difference[b]	1.44	1.85	0.0 (ref)	1.65 (0.48)[c]
sugar Q[d]				
A	0.35	0.38 ± 0.04	0.38 ± 0.01	0.38 ± 0.03
T	0.35	0.37 ± 0.03	0.38 ± 0.01	0.37 ± 0.02
sugar Ψ[e]				
A	191	144 ± 27	168 ± 3	144 ± 26
T	191	107 ± 33	153 ± 5	112 ± 26
helix repeat angle[f]	35.6	35 ± 3	39 ± 0.4	36 ± 3
glycosidic bond torsion angle				
A	82	59	74 ± 4	56 ± 13
T	82	46 ± 9	63 ± 4	46 ± 8
interbase twist[g]	4.2	18 ± 7	16 ± 8	18 ± 5
base tilt[h]				
A	5.9 ± 0.3	8 ± 3	6 ± 3	7 ± 2
T	6.0 ± 0.3	12 ± 4	10 ± 4	12 ± 4

[a] Total energy without distance constraints. Values in parentheses are with distance constraints included. [b] Root mean square difference between the given structure and the $B_{NMR/a}$ structure. [c] rms difference between $B_{RE/a}$ and $B_{NC/a}$ structures. [d] Out-of-plane amplitude of the sugar ring, as described by Cremer and Pople (1975). [e] Pseudorotation phase of the sugar ring, as described by Cremer and Pople (1975). [f] Average angle between successive bases, determined by the angles between the C1′–N glycosidic bonds on successive bases. [g] Defined as the angle between vectors normal to the planes of the paired bases. [h] Angle between the vector normal to the base and the helix axis.

Table III: Analysis of A-Form Structures for $(dA)_{10}\cdot(dT)_{10}$ Obtained from Combined Molecular Mechanics and Annealed Molecular Dynamics Calculations

structure/parameter	starting X-ray (A_{XRAY})	minimized, no constraints ($A_{NC/a}$)	minimized, 25-kcal constraints ($A_{NMR/a}$)	relaxed from 25-kcal constraints ($A_{RE/a}$)
energy (kcal/mol)		−567	−448 (−429)[a]	−574
rms structure difference[b]	3.26	2.48	0.0	2.24 (1.04)[c]
sugar Q[d]				
A	0.38	0.39 ± 0.01	0.36 ± 0.05	0.40 ± 0.02
T	0.38	0.40 ± 0.01	0.40 ± 0.02	0.38 ± 0.01
sugar Ψ[e]				
A	12	110 ± 20	167 ± 15	124 ± 15
T	12	52 ± 54	152 ± 8	104 ± 20
helix repeat angle[f]	28.5	29 ± 3	33 ± 2	30 ± 1
glycosidic bond torsion angle				
A	26	41 ± 4	81 ± 9	50 ± 15
T	26	33 ± 12	62 ± 6	45 ± 7
interbase twist[g]	11.7	7 ± 3	11 ± 3	8 ± 4
base tilt[h]				
A	16 ± 8	11 ± 5	13 ± 7	14 ± 9
T	16 ± 8	13 ± 4	8 ± 3	11 ± 7

[a] Total energy without distance constraints. Values in parentheses are for distance constraints included. [b] Root mean square difference between the given structure and the $A_{NMR/a}$ structure. [c] rms difference between $A_{RE/a}$ and $A_{NC/a}$ structures. [d] Out-of-plane amplitude of the sugar ring, as described by Cremer and Pople (1975). [e] Pseudorotation phase of the sugar ring, as described by Cremer and Pople (1975). [f] Average angle between successive bases, determined by the angles between the C1′–N glycosidic bonds on successive bases. [g] Defined as the angle between vectors normal to the planes of the paired bases. [h] Angle between the vector normal to the base and the helix axis.

Typically, the time required to minimize the energy of one structure was 5 min. In the molecular dynamics calculations, 2.5 ps required ~12 min (step size 1 fs).

Results

The results of the molecular mechanics calculations and the annealed molecular dynamics calculations are summarized in Tables I–IV. Coordinates for the starting structures (A_{XRAY}, B_{XRAY}, H_{XRAY}) were obtained from Arnott et al. (1972, 1983). For each structure the following set of calculations were carried out: (i) unconstrained energy minimization of the starting structure (yielding structures denoted A_{NC}, B_{NC}, and H_{NC}), (ii) energy minimization with NMR constraints (yielding structures denoted A_{NMR}, B_{NMR}, and H_{NMR}), and (iii) a second unconstrained energy minimization (yielding the relaxed structures denoted A_{RE}, B_{RE}, B_{RE}, and H_{RE}). In each calculation, the starting structure was the final structure from the preceding calculation. The set of nine structures obtained in

Table IV: Analysis of Heteronomous Form Structures of $(dA)_{10}\cdot(dT)_{10}$ Obtained from Combined Molecular Mechanics and Annealed Dynamics Calculations

structure/parameter	starting X-ray (H_{XRAY})	minimized, no constraints ($H_{NC/a}$)	minimized, 25-kcal constraints ($H_{NMR/a}$)[a]	relaxed from 25-kcal constraints ($H_{RE/a}$)
energy (kcal/mol)		−561	−546 (−537)	−577
rms structure difference[b]	1.84	(1.43)[d]	0.0	2.09 (0.95)[c]
sugar Q[e]				
A	0.45	0.37 ± 0.01	0.38 ± 0.01	0.38 ± 0.03
T	0.42	0.37 ± 0.02	0.38 ± 0.01	0.37 ± 0.01
sugar Ψ[f]				
A	7	65 ± 75	168 ± 5	140 ± 32
T	169	125 ± 25	152 ± 3	115 ± 35
helix repeat angle[g]	35.6	35 ± 3	39 ± 1	34 ± 3
glycosidic bond torsion angle				
A	26.5	40 ± 23	73 ± 5	57 ± 14
T	88	48 ± 8	56 ± 3	46 ± 11
interbase twist[h]				
A				
T	29	21 ± 4	16 ± 7	17 ± 7
base tilt[i]				
A	16	12 ± 6	6 ± 2	8 ± 3
T	18	10 ± 6	11 ± 4	12 ± 6

[a] Total energy without distance constraints in place. The value in parentheses is with the distance constraints included. [b] Root mean square difference between the given structure and the $H_{NMR/a}$ structure. [c] rms difference between $H_{RE/a}$ and $H_{NC/a}$ structures. [d] rms difference between H_{XRAY} and H_{NC}. [e] Out-of-plane amplitude of the sugar ring, as described by Cremer and Pople (1975). [f] Pseudorotation phase of the sugar ring, as described by Cremer and Pople (1975). [g] Average angle between successive bases, determined by the angles between the C1′–N glycosidic bonds on successive bases. [h] Defined as the angle between vectors normal to the planes of the paired bases. [i] Angle between the vector normal to the base and the helix axis.

Table V: Summary of rms Deviation of Observed Relaxation Rates and Those Calculated for Various Models of $(dA)_{10}\cdot(dT)_{10}$[a]

structure	rms, NMR (s^{-1})[b]	structure	rms, NMR (s^{-1})[b]
A_{NMR}	13	$B_{NMR/a}$	4.7
$A_{NMR/a}$	12.1	H_{NMR}	7.3
B_{NMR}	7.6	$H_{NMR/a}$	5.3

[a] These represent averages, for each structure, for the nine interactions calculated for the six central base pairs in the helix. [b] rms = $[\sum_{i=1}^{9} (R_i^{calcd} - R_i^{obsd})^2/9]^{1/2}$, where R_i^{obsd} = observed relaxation rate for interaction i and R_i^{calcd} is the corresponding rate calculated for the structure.

Table VI: Interproton Distances between AH2 and H1′ Sugar Protons in $(dA)_{10}\cdot(dT)_{10}$ (in Å)

	structure		
sugar residue[a]	B_{XRAY}	$A_{NMR/a}$	$B_{NMR/a}$ ($H_{NMR/a}$)
A_{-1}	6.7	6.8	6.8
A_0	4.7	4.6	4.6
A_1	5.5	4.9	4.9
T_{-1}	7.3	4.3	4.3
T_0	6.3	5.2	5.2
T_1	7.4	7.7	7.8

[a] 3′-A_1-A_0-A_{-1}-5′-5′-T_1-T_0-T_{-1}-3′.

Table VII: Summary of Minimum Internuclear Separation between Phosphate Atoms on Opposite Strands for A-, B-, and H-DNA and for the Corresponding $A_{NMR/a}$, $B_{NMR/a}$, and $H_{NMR/a}$ Structures

structure	minimum P–P separation (Å)	structure	minimum P–P separation (Å)
A_{XRAY}	17.0	$B_{NMR/a}$	10.9
$A_{NMR/a}$	12.9	H_{XRAY}	11.0
B_{XRAY}	11.7	$H_{NMR/a}$	10.6

the above series of calculations were then subjected to annealed molecular dynamics calculations, and these resulting structures are all denoted by the subscript a. Thus, $B_{NMR/a}$ represents the structure obtained by carrying out a minimization of the B form, including NMR constraints, and then subjected to annealing (with the NMR constraints in place). This sequence of calculations is shown schematically for B-DNA as

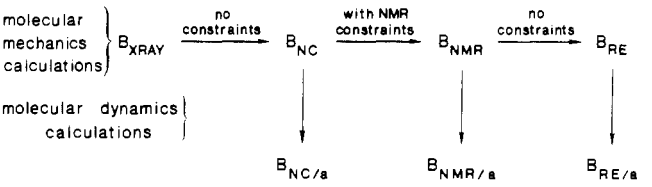

Information about the structural features of all the annealed structures is presented in Tables II–IV, and a comparison of the rms deviation between the observed NMR relaxation rates and those calculated for the various structures are presented in Table V. [For details of the rate calculations, please see Mirau et al. (1985) and Behling and Kearns (1986).] In Table VI we present distances between the AH2 protons and neighboring H1′ sugar protons and in Table VII the minimum interatomic separation between phosphorus atoms on opposite strands (minor groove width). Finally, in Table VIII we summarize the backbone torsional angles obtained for the $B_{NMR/a}$ structure.

Discussion

Before discussing the results of these calculations in terms of structural implications and relationship to the NMR measurements, we briefly consider other aspects of the cal-

Table VIII: Summary of Backbone Dihedral Angles[a] for the $B_{NMR/a}$ Structure of Poly(dA)·Poly(dT)

	dihedral angle (deg)					
nucleotide	ψ	ψ'	ϕ'	ω'	ω	ϕ
A	58 ± 1	146 ± 2	185 ± 2	242 ± 4	290 ± 2	178 ± 2
T	61 ± 1	137 ± 4	182 ± 2	250 ± 4	292 ± 2	176 ± 1

[a] ψ = O5′–C5′–C4′–C3′; ψ' = C5′–C4′–C3′–O3′; ϕ' = C4′–C3′–O3′–P; ω' = C3′–O3′–P–O5′; ω = O3′–P–O5′–C5′; ϕ = P–O5′–C5′–C4′.

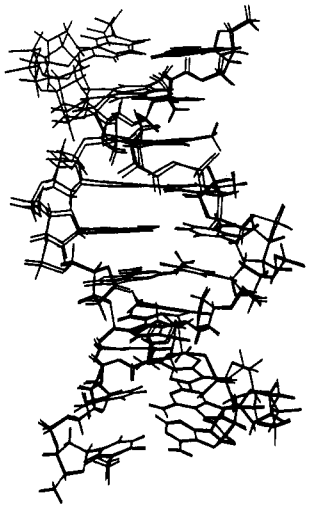

$B_{NMR/a}$, $H_{NMR/a}$

FIGURE 2: Comparison of the $B_{NMR/a}$ and $H_{NMR/a}$ structures showing that the energy minimization and annealed molecular dynamics calculations, including NMR constraints, cause the starting B_{XRAY} and H_{XRAY} structures to converge to a common structure.

culation. With the exception of the A_{NMR} structure, the annealed molecular dynamics calculations had relatively little effect on the energies of the various structures obtained from molecular mechanics calculations (see Table I). In the case of A_{NMR} the annealing process significantly lowered the energy, but even after annealing the resulting $A_{NMR/a}$ structure was still over 100 kcal higher in energy than the $B_{NMR/a}$ and $H_{NMR/a}$ structures. Inclusion of the NMR constraints in the energy minimization had the least affect in altering B-DNA, somewhat larger affects on H-DNA, and very pronounced affects on A-DNA. The resulting A_{NMR} and A_{RE} structures remain globally A form, but locally they are greatly altered. When the NMR constraints are removed, the final annealed structures ($B_{RE/a}$, $H_{RE/a}$, and $A_{RE/a}$) all have energies within 3 kcal of each other, but examination of the structural features given in Tables II–IV reveals that relative to the starting X-ray structures there have been major changes in the local structures of the A form, somewhat fewer changes in the H form, and little change in the B form. In all cases the conformation of the adenine sugars is C2′-endo or C1′-exo, whereas the thymine sugars all convert to C1′-exo.

The B_{NMR} and H_{NMR} structures have converged to nearly identical B-type structures (as have $B_{NMR/a}$ and $H_{NMR/a}$) (see Figures 2 and 3), but the A structure remains trapped in a structure that is globally A type. Ideally, molecular mechanics energy minimization with the NMR distance constraints would result in a structure that is independent of the starting DNA conformation. The results of these and other calculations (Kollman et al., 1982; Nilsson et al., 1986) show, unfortunately, that the resulting structures do depend on starting conformation. However, Nilsson et al. (1986) have shown that, using molecular dynamics with appropriate idealized constraints, A-DNA converts to B-form DNA and vice versa (Nilsson et al., 1986). In our case the NMR constraints with moderate annealed molecular dynamics was adequate to cause the starting H-DNA structure to convert to a B-type structure. It is likely that we would find the same result if we had run molecular dynamics over a longer time period on the A-DNA structure as did Nilsson et al. (1986). We now examine the results of the molecular mechanics and molecular dynamics calculations in light of the NMR measurements and structural implications.

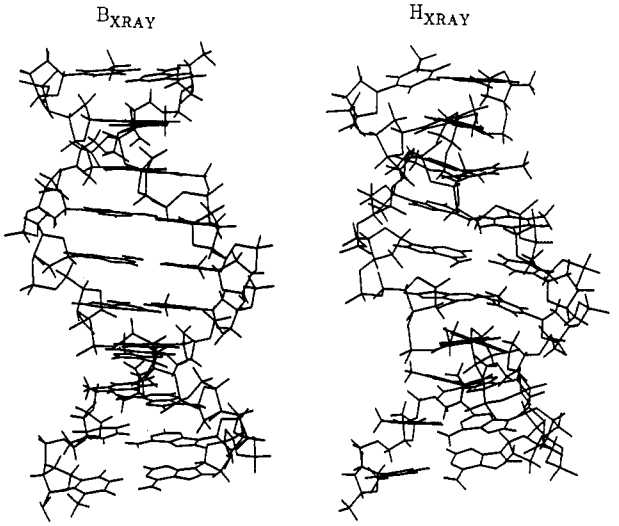

FIGURE 3: Comparison of the B_{XRAY} and H_{XRAY} starting structures illustrating the difference in the two structures.

The energy minimization and annealed molecular dynamics calculations that include the NMR constraints are expected to generate structures that give the best possible fits of the NMR data and, at the same time, are the best possible ones energetically. Because they give better fits of the NMR data and are energetically superior, we discuss only the structures arising from annealed molecular dynamics calculations that included the NMR constraints (i.e., $A_{NMR/a}$, $B_{NMR/a}$, and $H_{NMR/a}$). A summary of the rms deviation between the NMR relaxation rates calculated for the different structures and the observed rates in (Table V) demonstrates that the refinement procedure did lead to substantial improvements in all cases. Since, as noted above, the $H_{NMR/a}$ and $B_{NMR/a}$ structures are for all practical purposes the same, we only need to compare the $B_{NMR/a}$ and $A_{NMR/a}$ structures.

From Tables II–IV we see that all structures arising from annealed molecular dynamics calculations with NMR constraints have very similar backbone structures, nearly identical sugar puckers, albeit different global structures. All sugars are in the C2′-endo range, and glycosyl torsional angles are $\sim 75°$ for adenine and $\sim 62°$ for thymine. The helix repeat angle is 39° for B but 33° for the A form.

There are a number of important grounds for ruling out the $A_{NMR/a}$ structure relative to $B_{NMR/a}$ ($H_{NMR/a}$): (i) to satisfy the NMR constraints the $A_{NMR/a}$ structure is about 100 kcal higher in energy compared with the $B_{NMR/a}$ structure; (ii) the rms deviation between the observed and calculated relaxation rates is smaller by a factor of >2 for the $B_{NMR/a}$ structure than for the $A_{NMR/a}$ (see Table V); (iii) the observation (Behling & Kearns, 1986) that in the 2D NMR spectra of poly(dA)·poly(dT) the adenine H2 protons exhibit stronger ($\sim$ 2-fold) cross peaks with the *thymine* H1′ sugar protons on the opposite strand than with the adenine H1′ sugar protons on the same strand. The relevant interproton separations between the sugar H1′ and the AH2 proton are summarized in Table VI for the different structures obtained from the annealed molecular dynamics calculations. From these results we estimate that the predicted cross-peak intensity ratios, (AH2–TH1′)/(AH2–AH1′), would be 1.2 for both $B_{NMR/a}$ and $H_{NMR/a}$ and 0.18 for $A_{NMR/a}$ compared with an observed ratio of ~ 2. The cross-peak intensity ratio predicted for the $A_{NMR/a}$ structure is almost an order of magnitude smaller than the experimental value. The value calculated for the $B_{NMR/a}$ structure is not in perfect agreement with the observed results, but all that should be concluded from the experimental ob-

servations (due to the use of the 2D accordian technique) is that the interaction with the TH1′ sugar protons and AH2 is stronger than with the AH1′. Furthermore, the value calculated for the $B_{NMR/a}$ structure is very sensitive to the AH2–TH1′ separation, and a relatively small change (~10%) would bring the calculated value into agreement with the observed value.

It is clear from the above considerations that the $A_{NMR/a}$ structure can be rejected and that the results of the present calculation strongly point to a room temperature solution-state structure for poly(dA)·poly(dT) that is not very different from B-form DNA. Although the helix repeat angle is large (39° compared with 36°), this does not appear to have resulted in the unusually small minor groove that Drew and Travers proposed (1984, 1985). They noted that the minor groove width could range from 9 to 17 Å, depending upon the DNA conformation, and a comparison of the shortest interstrand phosphate–phosphate separation for the structures we examined is given in Table VII. The P–P separation is 11.7 Å in B_{XRAY} and 11.0 in H_{XRAY}, but in both $H_{NMR/a}$ and $B_{NMR/a}$ it has contracted only slightly to ~10.7 Å. This is a relatively small reduction in the minor groove width relative to standard B-DNA, and therefore our results do not provide much support for the Drew–Travers proposal. Perhaps unusual hydration in the minor groove of $(dA)_n$·$(dT)_n$ sequences is responsible for some of their special properties, including resistance to nucleases and to drug binding as proposed by Wilson et al. (1985).

The nature of the sugar puckering in poly(dA)·poly(dT) appears from our experiments to be mainly C2′-endo on both strands, although the thymine strand has a somewhat smaller average phase angle (152°) in $H_{NMR/a}$ and $B_{NMR/a}$ structures. Thus, it is clear that the structure suggested by Rao and Kollman, A(C2′-endo)·T(C3′-endo), as "competing" with standard B-DNA, A(C2′-endo)·T(C2′-endo), is closer to reality than the Arnott heteronomous structure, A(C3′-endo)·T(C2′-endo). When the constraints are removed ($H_{RE/a}$ and $B_{RE/a}$), the structure looks more like that proposed by Rao and Kollman (1985), not surprisingly, because the same molecular mechanics model was used.

Given the low barrier to sugar puckering in DNA, one can imagine equilibria of the sort A(C2′)·T(C2′) ⇄ A(C2′)·T(C3′) going on, but the results from $H_{NMR/a}$ and $B_{NMR/a}$ suggest the equilibrium is reasonably far to the left (90%:10%). Raman measurements on poly(dA)·poly(dT) gels indicate that this, as well as other DNAs, exist in an ~80%:20% mixture of C2′-endo and C3′-endo sugar conformation (Wartell & Harrell, 1986). It is hard to critically assess the accuracy of the various constraint distances and how well they would be fit by assuming equilibria of this sort, but it would be surprising if the percent C3′-endo found in this sequence turned out to be much larger than ~20%.

In considering the above results there are several points to remember. In addition to the intrinsic limitations of the current theoretical procedures, we note that the NMR data are limited in that they mainly include *local* interactions between the base and sugar protons and between sugar protons. These interactions are effective in establishing sugar puckers and glycosidic bond angles, but they are less effective in defining the positions of the bases relative to one another. In this study there is only one interaction between bases, the AH2–AH2 interaction, and this single interaction is not sufficient to drive the A-DNA structure over to the energetically more favorable B-DNA during the course of a molecular mechanics calculation. Inclusion of data on the relative strength of the AH2–H1′ interactions might have accomplished this. We also note that it will be difficult by NMR to detect the small amount of bending (~4–5° per A·T base pair) that is responsible for the unusual electrophoretic and hydrodynamic behavior of DNA containing in-phase A_5–T_5 sequences (Wu & Crothers, 1984; Levene et al., 1986).

Determination of a DNA structure using NMR distance constraints in molecular mechanics calculations is further complicated because the minimum energy structure gives a static picture of a low-temperature DNA structure, while DNA in solution at room temperature experiences large amplitude motions (Bolton & James, 1979; Hogan & Jardetzky, 1980; Levy et al., 1981; Mirau et al., 1985; Behling & Kearns, 1986). The NMR measurements are influenced by these motions, and a distance measured by NMR is a weighted average of the fluctuating interproton distance during the magnetic relaxation time of the proton. Using the distances determined from NMR relaxation rates as constraints in any molecular mechanics energy minimization or distance–geometry algorithm to determine a static structure may therefore give misleading results. It has been shown that the errors in the measured distance may be relatively small (Keepers & James, 1984; Clore & Gronenborn, 1985) and the error in resulting structure is probably minimized in the energy minimization calculation as compared to the distance–geometry approach because of other factors besides distances that are used in the calculation, but this difficulty must be remembered.

In view of the large amplitude motions present in solution-state DNA, and even in solid DNA (Shindo et al., 1980; Nall et al., 1981; Opella et al., 1981; Mai et al., 1983; Holbrook & Kim, 1984; Vold et al., 1986), it is perhaps unrealistic to talk about *the* structure of DNA. It is certainly reasonable to discuss the average structure, but we do not know at this point that our energy-minimized structure is the same as the time-average structure that would be obtained from a long-time molecular dynamics calculation. These calculations are currently in progress.

It is of interest to compare the results of our present study on poly(dA)·poly(dT) with the results of extensive restrained molecular mechanics and dynamics calculations on the hexamer $d(CGTACG)_2$ recently reported by Nilsson et al. (1986). In their work they used the CHARM program, which has an origin similar to the AMBER program. They too introduced constraints derived from NMR measurements with force constants that ranged from ~120 to 7.5 kcal, depending upon the error estimates in the NMR measurements. In our calculation we used a force constant of 25 kcal/mol for all interactions. Starting with either A-form DNA and using the molecular dynamics calculations, but with distance constraints for B-DNA (and vice versa), they found that A-DNA could be converted to B-DNA (and conversely) in less than 10 ps. This is reassuring since it shows that with sufficiently strong restraints the barrier to interconverting A- and B-DNA can be surmounted during a room temperature molecular dynamics simulation. However, in our work and that reported by Nilsson et al. (1986) using just molecular mechanics, the A → B DNA conversion does not occur. The structures obtained appears globally to be of the A type, but locally, they have sugar puckers and other structural features usually associated with B-DNA. Thus, with just the NMR constraints, the A–B interconversion does not occur during a molecular mechanics calculation.

Added in Proof

Alexeev et al. (1987) have recently reanalyzed the original data of Arnott et al. (1983) and concluded that it is better fit

by a structure that is much closer to B form than originally proposed.

ACKNOWLEDGMENTS

We are indebted to Dr. R. Hilderbrandt for helping with calculations performed on the San Diego Supercomputer. Funds for carrying out the computations were provided by the National Science Foundation. We acknowledge the use of the SDSC facility. The Chemistry Department computer graphics facility used in this research was supported, in part, by a grant from the National Science Foundation (DMB 84-00553). We thank Victor Hsu for helping with some of the computer graphics.

Registry No. $(dA)_{10}\cdot(dT)_{10}$, 86029-40-5.

REFERENCES

Alexeev, D. G., Lipanov, A. A., & Skuratovskii, I. Ya. (1987) *Nature (London) 325*, 821–823.

Arnott, S., & Hukins, D. W. L. (1972) *Biochem. Biophys. Res. Commun. 47*, 1506–1509.

Arnott, S., Chandrasekaran, R., Hall, I. H., & Puigjaner, L. C. (1983) *Nucleic Acids Res. 11*, 4141–4155.

Behling, R. W., & Kearns, D. R. (1985a) *Biopolymers 24*, 1157–1167.

Behling, R. W., & Kearns, D. R. (1985b) in *Book of Abstracts, Fourth Conversation in Biomolecular Stereodynamics* (Sarma, R. H., Ed.) p 79, Adenine, New York.

Behling, R. W., & Kearns, D. R. (1986) *Biochemistry 25*, 3335–3346.

Bolton, P. H., & James, T. L. (1979) *J. Phys. Chem. 83*, 3359–3366.

Clore, G. M., & Gronenborn, A. M. (1985) *J. Magn. Reson. 61*, 158–164.

Cremer, D., & Pople, J. (1975) *J. Am. Chem. Soc. 97*, 1354–1358.

Dickerson, R. E., Drew, H. R., Conner, B. N., Wing, R. M., Fratini, A. V., & Kopka, M. L. (1982) *Science (Washington, D.C.) 216*, 475–485.

Drew, H. R., & Travers, A. A. (1984) *Cell (Cambridge, Mass.) 37*, 491–502.

Drew, H. R., & Travers, A. A. (1985) *Nucleic Acids Res. 13*, 4445–4467.

Hogan, M. E., & Jardetzky, O. (1980) *Biochemistry 19*, 2079–2085.

Holbrook, S. R., & Kim, S.-H. (1984) *J. Mol. Biol. 173*, 361–388.

Jolles, B., Laigle, A., Chinsky, L., & Turpin, P. Y. (1985) *Nucleic Acids Res. 13*, 2075–2085.

Keepers, J. W., & James, T. L. (1984) *J. Magn. Reson. 57*, 404–426.

Klug, A., Rhodes, D., Smith, J., Finch, J. T., & Thomas, J. O. (1980) *Nature (London) 287*, 509–516.

Kollman, P., Keepers, J. W., & Weiner, P. (1982) *Biopolymers 21*, 2345–2376.

Kopka, M. L., Fratini, A. V., Drew, H. R., & Dickerson, R. E. (1983) *J. Mol. Biol. 163*, 129–146.

Leslie, A., Arnott, S., Chandrasekaran, R., & Ratliff, R. (1980) *J. Mol. Biol. 143*, 49–72.

Levene, S. D., Wu, H. M., & Crothers, D. M. (1986) *Biochemistry 25*, 3988–3995.

Levy, G. C., Hilliard, P. R., Levy, L. F., & Rill, R. L. (1981) *J. Biol. Chem. 256*, 9986–9989.

Mai, M. T., Wemmer, D. E., & Jardetzky, O. (1983) *J. Am. Chem. Soc. 105*, 7149–7152.

Marini, J. C., Levene, S. D., Crothers, D. M., & Englund, P. T. (1982) *Proc. Natl. Acad. Sci. U.S.A. 79*, 7664–7668.

McCammon, J. A., Gelin, B. R., & Karplus, M. (1977) *Nature (London) 267*, 585–590.

Mirau, P. A., Behling, R. W., & Kearns, D. R. (1985) *Biochemistry 24*, 6200–6211.

Nall, B. T., Rotwell, W. P., Waugh, J. S., & Rupprecht, A. (1981) *Biochemistry 20*, 1881–1887.

Nilsson, L., Clore, G. M., Gronenborn, A. M., Brunger, A. T., & Karplus, M. (1986) *J. Mol. Biol. 188*, 455–475.

Opella, S. J., Wise, W. B., & DiVerdi, J. A. (1981) *Biochemistry 20*, 284–290.

Pack, L., & Wang, J. (1981) *Nature (London) 292*, 375–378.

Pattabiraman, N. (1986) *Biopolymers 25*, 1603–1606.

Rao, S., & Kollman, P. A. (1985) *J. Am. Chem. Soc. 107*, 1611–1616.

Sarma, M. H., Gupta, G., & Sarma, R. H. (1985a) *J. Biomol. Struct. Dyn. 2*, 1057–1084.

Sarma, M. H., Gupta, G., & Sarma, R. H. (1985b) in *Books of Abstracts, Fourth Conversation in Biomolecular Stereodynamics* (Sarma, R. H., Ed.) p 77, Adenine, New York.

Shindo, H., Wooten, J. B., Pheiffer, B. H., & Zimmerman, S. B. (1980) *Biochemistry 19*, 518–526.

Sober, H. A., & Harte, R. A. (1970) in *CRC Handbook of Biochemistry*, pp H-18, H-19, The Chemical Rubber Co., Cleveland, OH.

Thomas, G. A., & Peticolas, W. L. (1983) *J. Am. Chem. Soc. 105*, 993–996.

Trifonov, E. N., & Sussman, J. L. (1980) *Proc. Natl. Acad. Sci. U.S.A. 77*, 3816–3820.

Vold, R. R., Brandes, R., Tsang, P., Kearns, D. R., Vold, R. L., & Rupprecht, A. (1986) *J. Am. Chem. Soc. 108*, 302–303.

Wartell, R. M., & Harrell, J. T. (1986) *Biochemistry 25*, 2664–2671.

Weiner, P., & Kollman, P. (1981) *J. Comp. Chem. 2*, 287–303.

Weiner, S. J., Kollman, P. A., Case, D. A., Singh, U. C., Ghio, C., Alagona, G., Profeta, S., & Weiner, P. (1984) *J. Am. Chem. Soc. 106*, 765–784.

Weiner, S. J., Kollman, P. A., Nguyen, D., & Case, D. (1986) *J. Comp. Chem. 1*, 230.

Wilson, W. D., Wang, Y. H., Krishnamoorthy, C. R., & Smith, J. C. (1985) *Biochemistry 24*, 3991–3999.

Woessner, D. E. (1962) *J. Chem. Phys. 37*, 647–654.

Woessner, D. E., Snowden, B. S., & Meyer, G. H. (1969) *J. Chem. Phys. 50*, 719–721.

Wu, H. M., & Crothers, D. M. (1984) *Nature (London) 308*, 509–513.